CHAPTER V
MORPHOLOGY DEVELOPMENT AND STABILITY OF POLYPTOPYLENE/ORGANOCLAY NANOCOMPOSITES

5.1 Abstract

A series of polypropylene (PP)/organoclay nanocomposites with varied concentrations of clay, from 1 to 7 wt%, was successfully prepared via melt intercalation using a PP functionalized with maleic anhydride as compatibilizer. The morphology/property relationships of the nanocomposites were investigated by XRD, TGA, and DSC analyses. Two distinct groups of composites, from a quasi-exfoliated to an intercalated morphology, were identified. In particular, intercalated/flocculated morphologies were obtained for those composites with an organoclay concentration beyond the threshold (3 wt%), as evidenced by XRD analysis and confirmed by an increase in the glass transition temperature. This last effect was related to the confinement of polymer chains between the silicate layers, generating a reduction of the chain mobility. The variable increase of the thermal stability of the nanocomposites was also likely related to the different degrees of exfoliation/intercalation of the samples. The toluene extraction of composites having a semi-exfoliated structure split the samples into two fractions having a similar morphology; for those samples having the higher organoclay concentration and intercalated morphology, a toluene-residue fraction containing almost all of the clay was obtained. Furthermore, in this case, the morphology analysis of the residue fraction evidenced a collapse of the inorganic structure compared to that of the unextracted composite. A careful characterization of both soluble and residue fractions is reported and the results are discussed considering the interactions at the interface between the functionalized PP chains and the silicate layers, and their effects on the organoclay dispersion state and stability.

(**Key-words**: polyolefins; nanocomposites; nanoconfinement; morphology; interfacial interaction; solvent fractionation)

5.2 Introduction

Polymer/clay nanocomposites are a class of hybrid materials composed of an organic polymer matrix in which inorganic nanoscale particles are imbedded (Messersmith, 1995; Usuki, 1993; Kojima, 1993; Yano, 1993; Vaia, 1995; Biasci, 1994). At this scale, the inorganic fillers dramatically improve the physical and mechanical macroscopic properties of the polymer, even when their amount is low (< 3–5% wt). In particular, polymer nanocomposites prepared by using layered inorganic substrates exhibit high heat distortion temperatures, enhanced flame resistance, increased modulus values, improved barrier properties, and decreased thermal expansion coefficient (Giannelis, 1996 and Wang, 1998). The enhanced properties are presumably due to the synergistic effects of the nanoscale structure and the particle–particle interactions extended to the polymer surfaces.

Beyond the conventional phase-separated polymer/clay composites, two ideal types of nanocomposites are possible. Intercalated structures are formed when a single (or sometimes multiple) extended polymer chain is intercalated between the silicate layers. The result is a well ordered multilayer structure of alternating polymer and inorganic layers, with a repeated distance between them. The intercalation causes a less than 2–3 nm separation between the layers (Alexadre, 2000; Chin, 2001; Kim, 2001). On the other hand, exfoliated or delaminated structures can be obtained when the clay layers are well separated each from other and individually dispersed in the continuous polymer matrix (Alexadre, 2000; Chin, 2001; Kim). In this case, the polymer expands the clay layers to 8–10 nm or more (Kim *et al.* 2001). That is, the interlayer expanse is comparable to the radius of gyration of the polymer rather than to that of an extended chain, in the intercalated hybrids (Giannelis *et al.* 1996). The exfoliation configuration is of particular interest because it maximizes the polymer–clay interactions making the entire surface of the layers available for the polymer. This leads to the most significant changes in the mechanical and physical properties (Dennis *et al.* 2001). However, it is not easy to achieve complete clay exfoliation and, with few exceptions, the majority of the polymer nanocomposites reported in the literature have intercalated or mixed intercalated/exfoliated nanostructures (Chin *et al.* 2001).

Most of the work reported in literature has focused on the importance of the "chemistry" used to modify the surface of the clay, usually montmorillonite (MMT), to favor the thermodynamics and kinetics (Vaia, 1995 and 1997; Manias, 2000) involved in melt intercalation, maximizing the effective interactions and leading to the above-mentioned morphology and properties. In particular, the surface modification of clay by surfactants and the use of specifically functionalized compatibilizers (grafted and/or block copolymers) were extensively employed as suitable methodologies to address the morphology properties toward high levels of nanodispersion by taking advantage of van der Waals and polar interactions predicted by using Hamaker constants (Hamaker, 1937). Indeed, the Vaia tractable approach (Vaia and Giannelis, 1997) reports that a "favorable enthalpy of mixing is achieved when the polymer/filler interactions are more favorable than the surfactant/filler interactions". This suggests that an appropriate design of the nanocomposite structure can be approached by modulating the interface and particularly the interfacial interactions mostly associated with the competitive adsorption of polymer and surfactant between the clay platelets.

More recently, thermodynamic and dynamic factors were simultaneously tuned for controlling the morphology development during melt intercalation. Moreover, the role and importance of material processing, and the interplay between the thermodynamics and shear, was also assessed (Dennis, 2001; Cho, 2004; Wang, 2004).

Recent studies about the relationships between morphology and mechanical response and/or thermal behavior took into account that the polymer chains close to the interface are located in a 'constraint region' surrounding the nanoscopic filler; that is expected to differ in properties and morphology from the bulk polymer matrix. Indeed, significant variations of polymer properties, have been experimentally observed, especially the glass transition temperature (T_g), owing to the different flexibility and mobility of macromolecules trapped on the surfaces of nanoparticles or confined between the silicate layers.

The phenomenon of chain confinement is still a subject of scientific controversy. Several methods such as dynamics simulation, models, and experiments about intercalation or capping of nanoparticles for interacting or non-interacting

nanofiller–polymer systems have been used to prove that the T_g of confined chains in polymer nanocomposites is changed (depressed or enhanced) (Giannelis, 1999; Vaia, 1997; Elmahdy, 2006; Anastasiadis, 2000) depending on the kind of polymer and its thermal properties, the presence of surfactants, the amount of inorganic filler, and obviously the morphology of the nanocomposities. With specific reference to nanostructured layered silicate materials (i.e. montmorillomite, MMT), intercalated polyethylene oxide (PEO)/MMT nanocomposites showed very fast relaxations associated with a low T_g value, thus indicating that the cooperative motion precipitously decreases as the polymer is confined to extremely narrow slits, less than a few nanometers (Vaia *et al.* 1997). Later, dielectric spectroscopy experiments showed that the confinement of PEO in sodium montmorillonite results in a speed-up of the PEO segmental relaxation dynamics, enhancing the ionic mobility of the nanocomposites (Elmahdy *et al.* 2006). Similar results were reported for polymethylphenylsiloxane–forming intercalated hybrids with organically modified layered silicate (OMMT) (Anastasiadis *et al.* 2000). On the other hand, the dynamic mechanical analysis of poly(methyl methacrylate) (PMMA)/MMT nanocomposites prepared by *in situ* intercalative polymerization showed an increase of the T_g with growing clay content, compared to the pure polymer. The authors proposed that part of the PMMA chains in the nanocomposites was strongly interacting with the inorganic surfaces and/or were trapped between the layers, hence being resistant to PMMA common solvents and suggesting that the nanoconfinement can change the macromolecule solubility (Li *et al.* 2003).

Polyolefins, due to their hydrophobic nature, are not able to establish interface interactions so effectively as to disperse the nanoparticles by intercalation and stabilize the morphology; for this reason, suitable surfactants as inorganic surface modifiers and functionalized polyolefins as matrix or as compatibilizers are generally used: the combined hydrophobic and hydrophilic interactions grant both the effects, even if the concentration/amount of polar groups is very low, generally less than 1% by mol (Ciardelli, 2008; Passaglia, 2005 and 2008). In this way, the preparation of polyolefin nanocomposites with a well-established dispersion level reflected in good performances (particularly for gas barrier properties) is possible and well-documented in the literature (Ciardelli, 2008; Passaglia, 2005 and 2008).

The thermal analysis of these samples generally highlights that the cooperative relaxation of polyolefin chains in the composites becomes weak due to the restricted mobility of the chains in the presence of clay platelets (Hambir *et al.* 2001). Moreover, solvent extraction procedures allowed for the isolation of polyolefin chains strongly interacting and/or trapped between the layers with a T_g (determined by DSC and assessed also by dielectric measurements) higher than that of the bulk matrix (Passaglia *et al.* 2008). More recently, a theoretical approach, reasonably explaining some important features and results (particularly about the mechanical and rheological behavior of polypropylene(PP)/clay nanocomposites), evidenced that when the organoclay amount is higher than 2% by weight, a three-dimensional filler network is formed and it plays an essential role in the dynamics behavior of the PP chains. The physical jamming and connecting of the nanoscale dispersed fillers (randomly oriented clay tactoids with locally correlated layers) generates a structure larger than that of intercalated and exfoliated microstructures; this larger structure can be regarded as a mesoscopic structure where motion of the PP chains is restricted (Wang *et al.* 2006).

By considering that PP is one of the most widely used commodity thermoplastics for preparing polymer/clay nanocomposites with conventional melt-mixing technology (Xu *et al.* 2003), we are reporting here results on the morphology/property relationships of PP/organoclay nanocomposites obtained with increasing amounts of organoclay (from 1 to 7 wt%). The development/establishment of exfoliated, intercalated and even mesoscopic structures as a function of the organoclay content was evidenced by combining XRD, TEM, and a solvent fractionation procedure. The extraction of polyolefin nanocomposites with a solvent dissolving the polymer allows for the separation of free polymer chains from those chains strongly interacting with lamellae; this strong interaction causes these chains to be insoluble in the solvent (Passaglia, 2001 and 2008). This analysis, which is not generally used, represents a powerful method to provide evidence for polymer/clay interface interactions and it is also a good way to isolate the adsorbed/interacting nanoconfined polymer from the non-intercalating macromolecules. Thus, the macroscopic/bulk properties of toluene soluble and insoluble composite fractions were investigated and compared with those of the starting materials (polymers, clay,

and composites). Moreover, in order to evaluate and correlate the change of polymer properties to different morphologies (confinement effects), infrared spectroscopy measurements (IR) and thermal analysis (DSC, TGA) were also carried out. A major emphasis was placed on understanding the role of organoclay nanodispersed platelets on composite properties before and after the extraction procedure, thus contributing to further clarifying the open questions concerning these interacting materials.

5.3 Results and Discussion

5.3.1 Morphology of PP/organoclay nanocomposites

The XRD patterns of the nanocomposites (Figure 5.1) clearly showed a shift of the OBTN (001) diffraction peak toward lower angles for all of the samples, which were prepared by adding different amounts of organoclay (ranging from 1 to 7% wt), indicating an increase of the interlayer spacing (d_{001}) by the intercalation of the polymer chains. Nevertheless, some differences (i.e. position, shape, and intensity of the d_{001} peak), were observed moving from the lower to the higher OBTN content. In the case of PP composites containing 1, 2, and 3 wt% OBTN, the d_{001} peak position was consistent with an interlayer spacing of 3.4 nm, thus indicating the probable formation of an intercalated structure even though the presence of single lamella can not be confirmed. The 5 and 7 wt% OBTN composites on the other hand , showed two distinct d_{001} peaks: one at lower angle, which was consistent with a d_{001} of 3.2 nm, and a second peak at the same (001) reflection angle of the pure OBTN (or weakly higher). As already reported and discussed in literature (Ciardelli, 2008; Passaglia, 2008; Wang, 2006), for high amounts of organoclay and/or by increasing its content, a considerable aggregation (tactoids and macro-aggregates) of the layers in polyolefin nanocomposites is generally observed (Causin, 2005 and Preschilla, 2008). Accordingly, also in this case, the addition of more OBTN enhanced the density of clay stacks and layers in the PP matrix, thus resulting in a strong connection between tactoids, layers, and polymer chains. The final effect is the gradual formation of a "percolating filler network structure" as the clay content reaches a certain threshold. Indeed, in our previous work, a threshold value of the organoclay content (3 wt% OBTN) was observed, beyond which a significant change

of the shear stress/viscosity and flow activation energy (E_a) behavior took place (Muksing *et al.* 2008). This result is consistent with the formation of a mesoscopic or percolating filler network structure, in agreement with the morphological analysis: the formation of intercalated structures and the increase of clay concentration favored the interactions between clay tactoids, clay layers, and polymer chains.

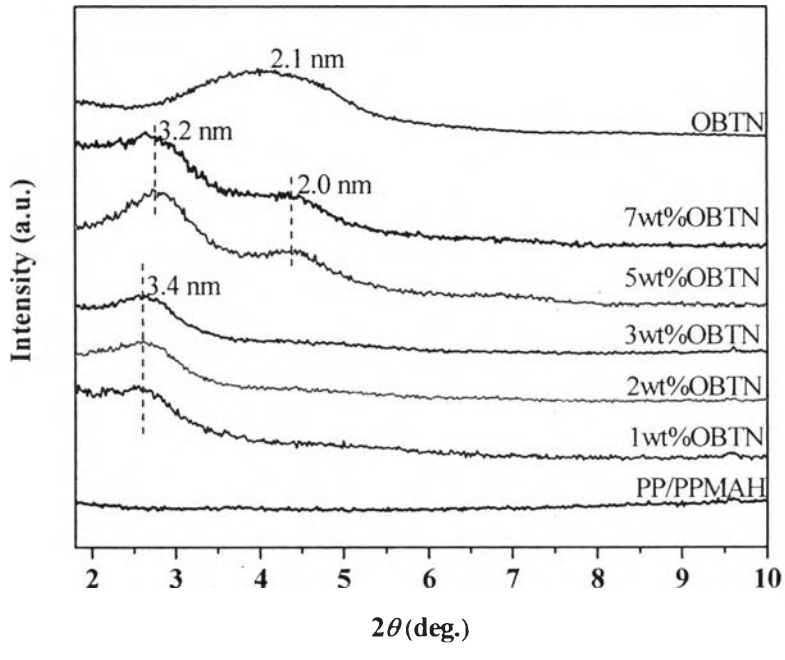

Figure 5.1 XRD patterns of PP/organoclay nanocomposites at various OBTN contents.

5.3.2 Thermal properties of PP/organoclay nanocomposites

Figure 5.2 shows the crystallization thermograms of PP/organoclay nanocomposites at various OBTN contents. The melting and crystallization temperatures (T_m and T_c, respectively), as well as the melting enthalpy (ΔH_m) and degree of crystallinity (χ_c), calculated from the second heating run, are summarized in Table 5.1. The 1 wt% OBTN nanocomposite showed the maximum T_c and degree of crystallinity (χ_c). Further increasing the organoclay content, particulay above 3 wt%, a slightly decrease of both the T_c and χ_c was produced. Nevertheless, for all the nanocomposites, the χ_c was higher than that of the matrix (PP/PPMAH blend)

moving from 48.6% to 49.7%, even if the T_m was not significantly influenced (Table 5.1). From the DSC thermograms, it was also observed that for the higher organoclay content (≥ 3wt% OBTN, which is the percolating filler threshold) (Muksing *et al*, 2008), the T_c shifted toward lower values, which is consistent with the confinement of polymer chains between the layers, causing a decrease of the crystallization rate (Lincoln, 2001; Perrin-Sarazin, 2005; Yuan, 2006).

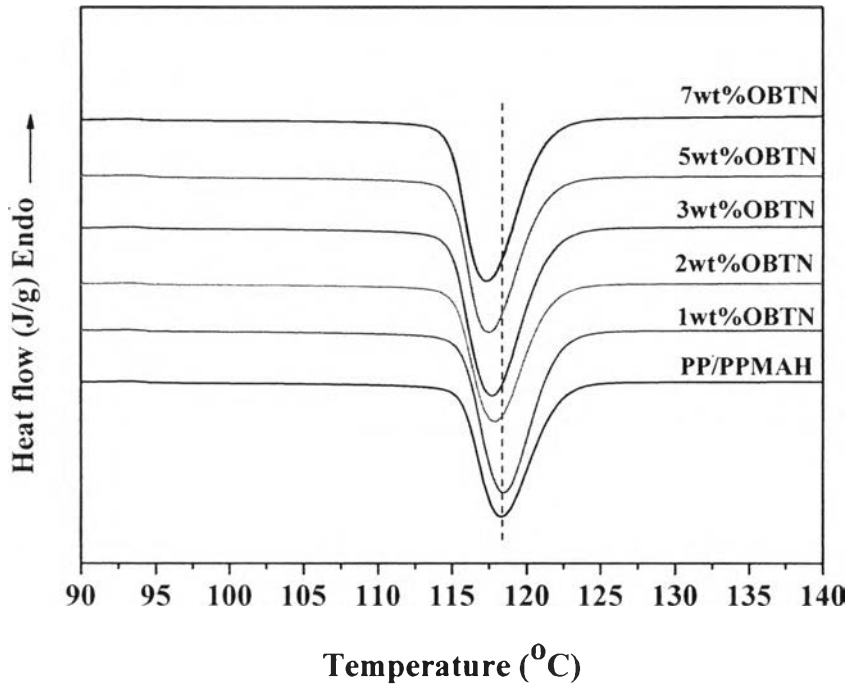

Figure 5.2 Crystallization thermograms of PP/organoclay nanocomposites at various OBTN contents.

The glass transition temperature (T_g) of the nanocomposites obtained by DSC analysis (Figure 5.3 and Table 5.1) was higher than that of the matrix, thus confirming the existence of good polymer–filler interactions reducing the mobility of the polymer chains. Interestingly, both the T_g and the nanocomposite morphology seem to be influenced by the amount of added clay Indeed, the T_g generally increases by decreasing the filler particle size (from micro to nano), owing to the enhanced polymer–filler interaction area. The nanocomposite containing 1 wt% OBTN exhibited the lowest T_g (5.9 °C), which is 1.7 °C higher than that of the pure

matrix, while the highest T_g value was obtained for the 5 wt% OBTN nanocomposite (9.8 °C). In fact, in this last case, by combining the XRD results and capillary rheology behavior (Muksing *et al.* 2008), it can be established that this sample has a predominantly intercalated morphology with evidence of a percolated filler network structure that strongly raises the average contact surface area between the polymer and filler. The confinement of polymer chains probably generates a reduction of the chain mobility until there is suppression of cooperative segmental motions of the confined macromolecules, thus determining an increase of the T_g. Moreover, the percolated filler network could also be responsible of a further restriction of chain mobility (Passaglia, 2008 and Wang, 2006).

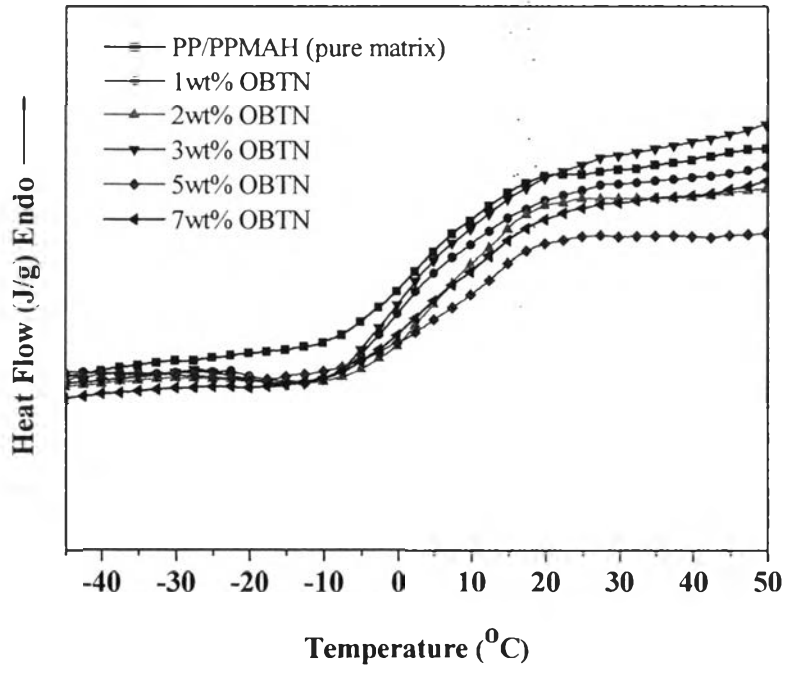

Figure 5.3 DSC thermograms of PP/organoclay nanocomposites at various OBTN contents: determination of the glass transition temperature (T_g).

Table 5.1 DSC and TGA results of PP/PPMAH and PP/PPMAH/organoclay nanocomposites at various OBTN contents

Composition (PP/PPMAH/%Organoclay)	T_c peak (°C)	T_m peak (°C)	ΔH_m[a] (J/g)	χ_c[b] (%)	T_g[c] (°C)	$T_{10\%}$[d] (°C)	$T_{50\%}$[d] (°C)	Residue[e] (%)
85/15/0	118.3	162.4	69.8	46.8	4.2	300.7	356.9	-
84/15/1wt%OBTN	118.5	163.2	75.4	49.1	5.9	294.5	387.5	1.2
83/15/2wt%OBTN	117.8	162.7	74.2	49.7	8.9	319.1	396.5	1.5
82/15/3wt%OBTN	117.6	163.0	71.6	48.5	6.5	340.2	406.2	2.3
80/15/5wt%OBTN	117.5	162.5	70.1	48.1	9.8	322.8	397.4	4.1
78/15/7wt%OBTN	117.3	162.9	70.6	47.5	7.0	350.5	417.3	3.2

[a]Measured on the second heating curve.

[b]Calculated as follows: $\chi_c=[A_c/(A_c+A_a)]*100$ (Machado *et al.* 2005), where A_c is the sum of all Bragg's reflection areas and A_a is the area of the amorphous halo.

[c]Glass transition temperature (T_g) of the nanocomposites calculated in the range of -10°C and 30 °C in the second heating curve.

[d]$T_{10\%}$ and $T_{50\%}$ are the temperatures relative to mass loss of 10 and 50 %wt, respectively,

[e]Char residue at 900 °C obtained from TGA analysis.

The thermal stability of PP/organoclay nanocomposites was checked by TGA (Figure 5.4 and Table 5.1), evidencing a remarkable improvement at both lower and higher temperatures as compared with the neat matrix. Indeed, the temperatures corresponding to 10% and 50% of the weight loss ($T_{10\%}$ and $T_{50\%}$) for all the nanocomposites were shifted higher with increasing organoclay content. In this case, there seems to be a combination of two effects: the amount of added clay and the morphology of the nanocomposite. At a relatively low organoclay content, the initial thermal stability increases with increasing OBTN content. In fact, the nanocomposite with 3 wt% OBTN showed the highest thermal stability, similar to that of the composite containing 7 wt% organoclay. Instead, in the case of the sample prepared with 5 wt% OBTN, the thermal stability decreased. This may be due to the presence of non- intercalated OBTN tactoids, which are less effective in blocking the heat transfer than single layers or intercalated tactoids.

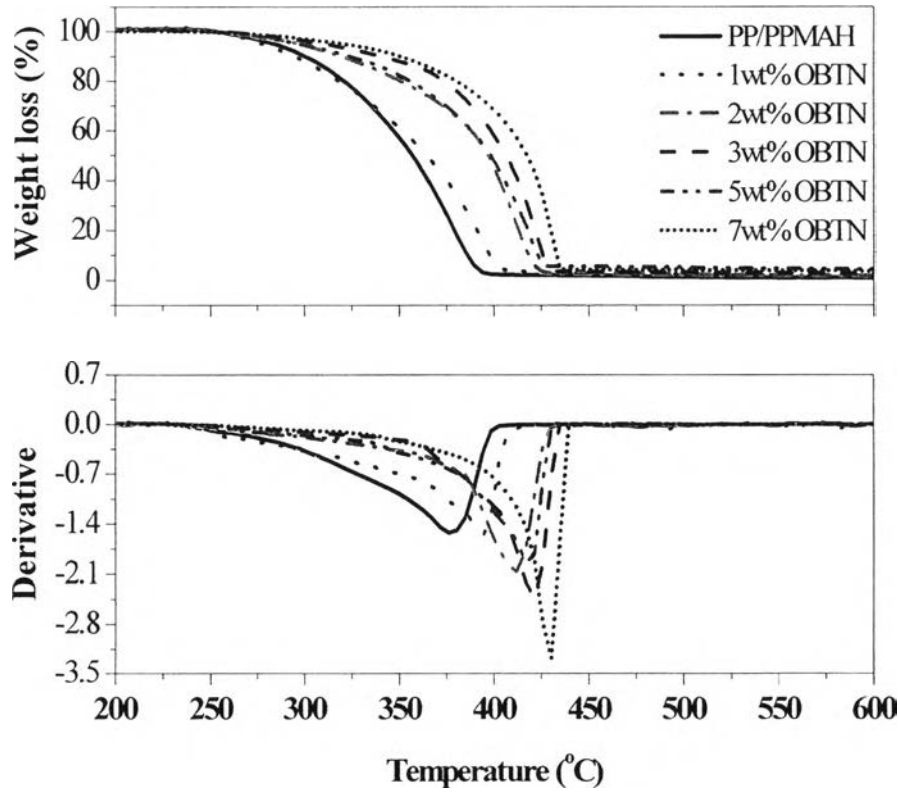

Figure 5.4 TGA (top) and DTG (bottom) thermograms of PP/organoclay nanocomposites at various OBTN contents.

5.3.3 Fractionation of PP/organoclay nanocomposites by solvent extractions

The solvent extraction technique was used in order to investigate the nanocomposite structural stability and the role of the interfacial interactions between layered silicate and polymer (Li, 2003; Passaglia, 2001 and 2008). A solvent able to completely dissolve the original polymer is generally chosen in order to separate free polymer chains from polymer chains strongly interacting with lamellae that should be insoluble (Passaglia *et al.* 2008). Despite the fact that the isotactic PP used in this work is completely soluble in refluxing xylene, both the polymer chains and the layered silicates were indiscriminately extracted for all PP/organoclay nanocomposites, except for the composite containing 7 wt% OBTN (Table 5.2). Most likely, this effect was due to the capability of xylene to promote the organoclay delamination (Ho and Glinka, 2003), thus reducing particle dimensions and allowing the lamellae extraction from the stainless steel net. Only for the highest OBTN content (7 wt%), was possible to recover a low amount of insoluble material (4 wt%), which was composed of both polymer and filler, as shown by FTIR and XRD analyses (Figure 5.5 and Figure 5.6).

Indeed, the FTIR spectrum evidenced absorption bands of PP at 1462 and 1375 cm^{-1} and signals owing to the OBTN at around 3500 and 1000 cm^{-1}. The XRD pattern also showed a reflection at low angles corresponding to the clay and 2θ reflections between 13° and 30°, characteristic of PP.

Consequently, the samples were extracted with boiling toluene, rather than xylene, even though the matrix (PP/PPMAH blend) is not completely soluble in this solvent (Table5.2). It has been reported that the isotactic PP solubility in hot toluene is influenced by the polymer crystallinity and it is believed that only the amorphous part is soluble (Li *et al.* 2003). In addition, it was also found that the PP/PPMAH blend gives a higher amount of residue than the pure PP (ca. 25 wt%). This last effect might be caused by chain interaction such as the hydrogen bonding between hydrolyzed maleic anhydride grafted PP groups, affecting the solubility and the crystallinity of the PP. It has already been demonstrated that the functional grafted groups influence the crystallization of PP, reducing the homogeneous nucleation at high cooling rate, and acting as a heterogeneous nucleating agent

(Krump, 2006 and Seo, 2000). In our case, the T_c of pure PP was 113.6 °C while the T_c of the PP/PPMAH blend was about 5 °C higher (118.3 °C), but the percentage of crystallinity of the PP/PPMAH blend calculated by XRD (Table 5.1) was slightly lower than that of the pure PP (46.8 % vs. 47.3%).

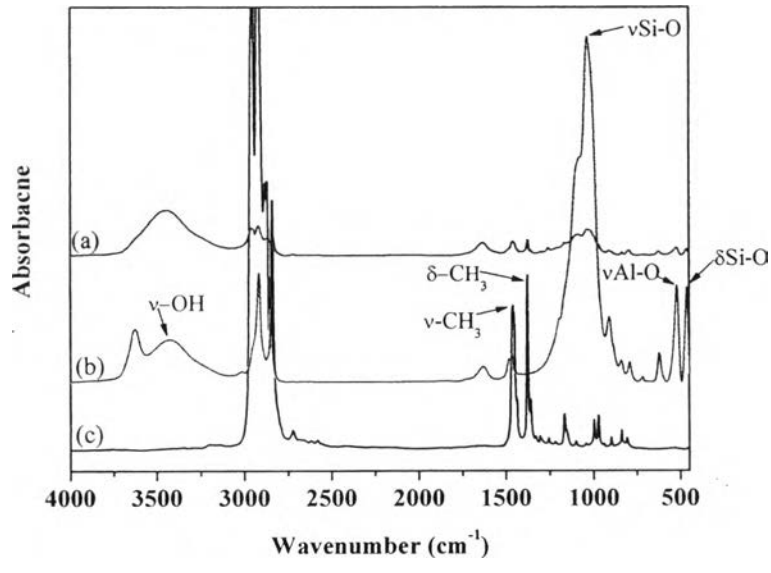

Figure 5.5 FTIR spectra of (a) 7 wt% OBTN nanocomposite xylene-residue, (b) OBTN organoclay, and (c) PP/PPMAH blend.

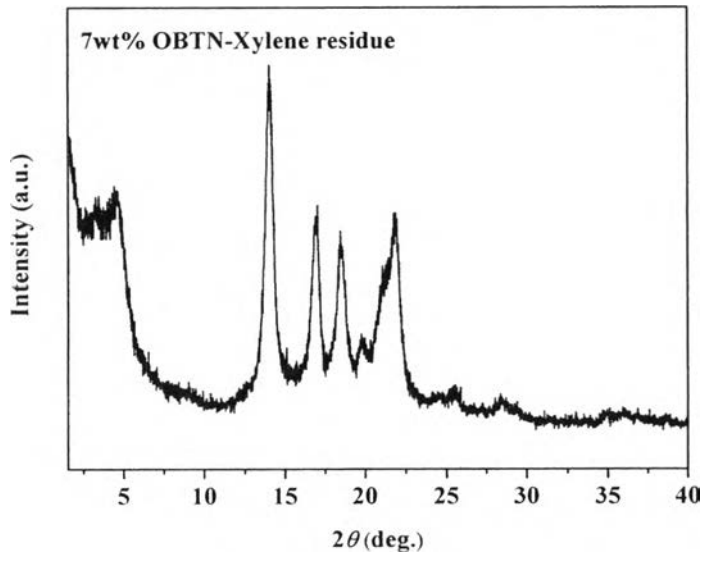

Figure 5.6 XRD pattern of the 7wt% OBTN nanocomposite xylene-residue fraction.

For all the composites, a higher amount of insoluble material than that of the pure matrix was obtained and only was partially proportional to the amount of the organoclay. Like in the case of functionalized EPM composites prepared with silica and organo-montmorillonite (Passaglia, 2001 and 2008), an increase of the percentage of insoluble polymer with increasing filler concentration should be connected to the strong interactions between the inorganic substrate and the polymer chains. Indeed, the interactions occurring between the polymer and the silicate surface are able to immobilize polymer chains inside and/or on the surface of the layered silicate. However, it cannot be excluded that the increase of the crystallinity degree, observed for all the nanocomposites, also influenced the extraction results. Hence, the soluble fractions might theoretically consist of soluble PP chains, while the residue fraction should consist of: (i) a toluene insoluble PP fraction and (ii) a polymer/clay fraction where polymer chains are confined between the silicate layers or are strongly interacting. The presence of an inorganic phase in the toluene residues was also confirmed by TGA analysis, showing a remarkably higher content of TGA residue with respect to the soluble parts for all the composites. To collect more evidence supporting the distribution of both components in the soluble and residual fractions, FTIR spectra were recorded.

The FTIR spectra of all the residue fractions (Figure 5.7(a)) showed the characteristic peaks of both PP and layered silicate. The absorption peaks at 3630, 1040, and those between 600 and 400 cm^{-1} can be associated respectively to the –OH stretching of the lattice water, Si–O stretching, and Al–O and Si–O bending, respectively (Zhang *et al.* 2004). Concurrently, peaks at 1456 ($-CH_3$ asymmetry stretching), 1376 ($-CH_3$ symmetry bending), 1163 ($-CH_3$ rocking), 975 ($-CH_2$ rocking), 853 ($CH-CH_2$ stretching), and 812 cm^{-1} ($CH-CH_3$ stretching) are characteristic of PP (He *et al.* 2003). In the case of soluble fractions (Figure 5.7(b)), although all the FTIR spectra showed peaks mainly due to PP, weak signals at 1040 and 600–400 cm^{-1} confirmed the presence of a low amount of the filler in these fractions also.

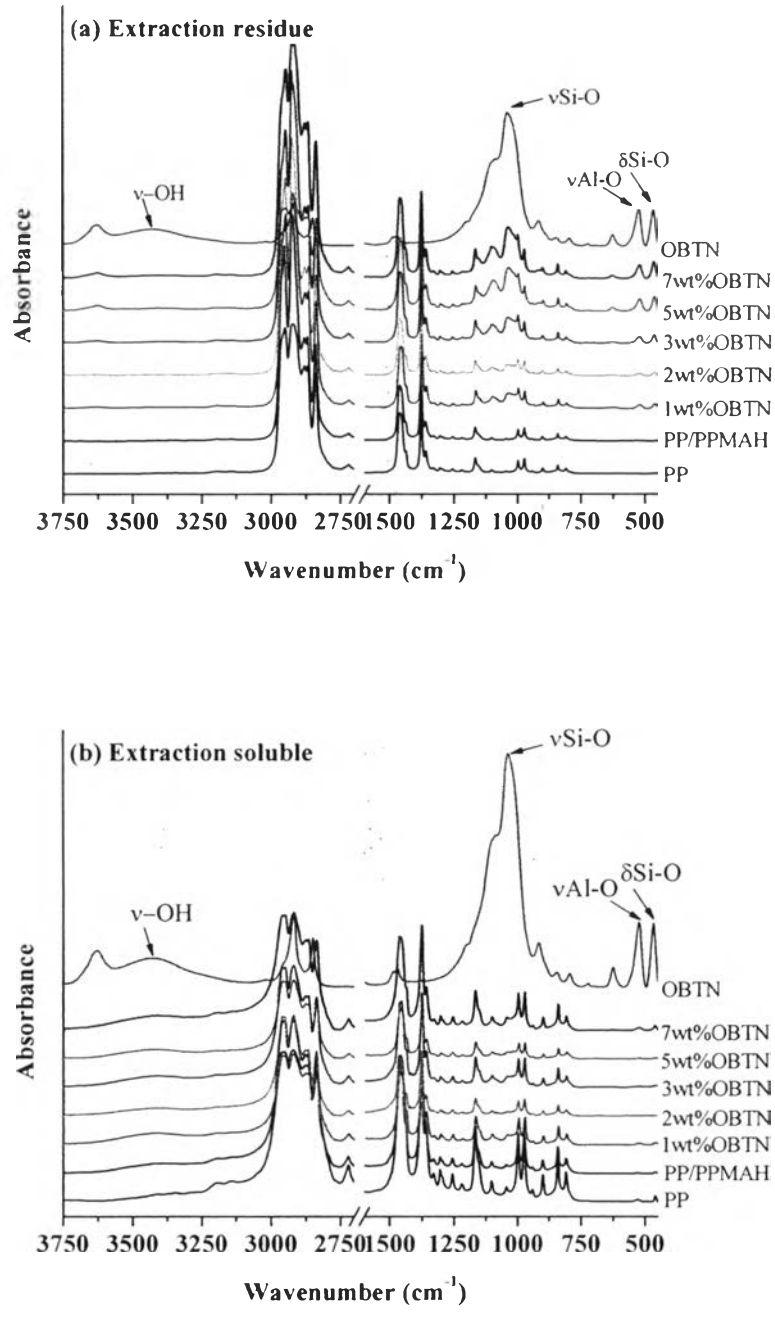

Figure 5.7 FTIR spectra of the (a) soluble fractions and (b) residues of PP/organoclay nanocomposites at various OBTN contents.

The XRD analysis of both the residues fractions and soluble fractions (Figure 5.8(a) and 5.8(b)) of samples containing 1 and 2 wt% OBTN, respectively, showed the disappearance of the (001) reflection peak at $2\theta = 2.7°$ ($d_{001} = 3.4$ nm), which was representative of the unextracted nanocomposite, thus indicating a more disordered structure of the clay due to the extraction process, as though a partial further exfoliation of the pristine structure occurred during the extraction. A similar result was obtained for the 2 wt% OBTN sample, which showed a weak broad peak at $2\theta = 4.47°$ ($d_{001} = 1.98$ nm) only in the residue. A completely different behavior was observed for the 3, 5, and 7 wt% OBTN composites: the residue fractions of these nanocomposites evidenced the presence of two peaks corresponding to an interlayer spacing of 2.4–2.8 and 1.7–1.9 nm, respectively; on the other hand the soluble fractions seemed completely exfoliated or quasi-exfoliated. Compared to the starting composite, the toluene extraction caused a separation between two compositionally/morphologically different phases: a soluble fraction, containing a low amount of inorganic layered silicate characterized by a very good dispersion providing an exfoliated morphology; and an insoluble fraction, containing the main percentage of the starting amount of silicate characterized by an intercalated morphology, and probably stacks and tactoids of unmodified OBTN. This result demonstrates that the morphology of the PP/OBTN nanocomposites prepared with a high amount of organoclay is not completely stable and, by extraction, a collapse of the organoclay layered structure is observed. This effect is presumably due to the removal of polymer chains confined between the silicate layers and probably not effectively interacting with the clay surface (Passaglia *et al.* 2008); however, it cannot be excluded that there is a possible desorption of the physically adsorbed organic surfactant.

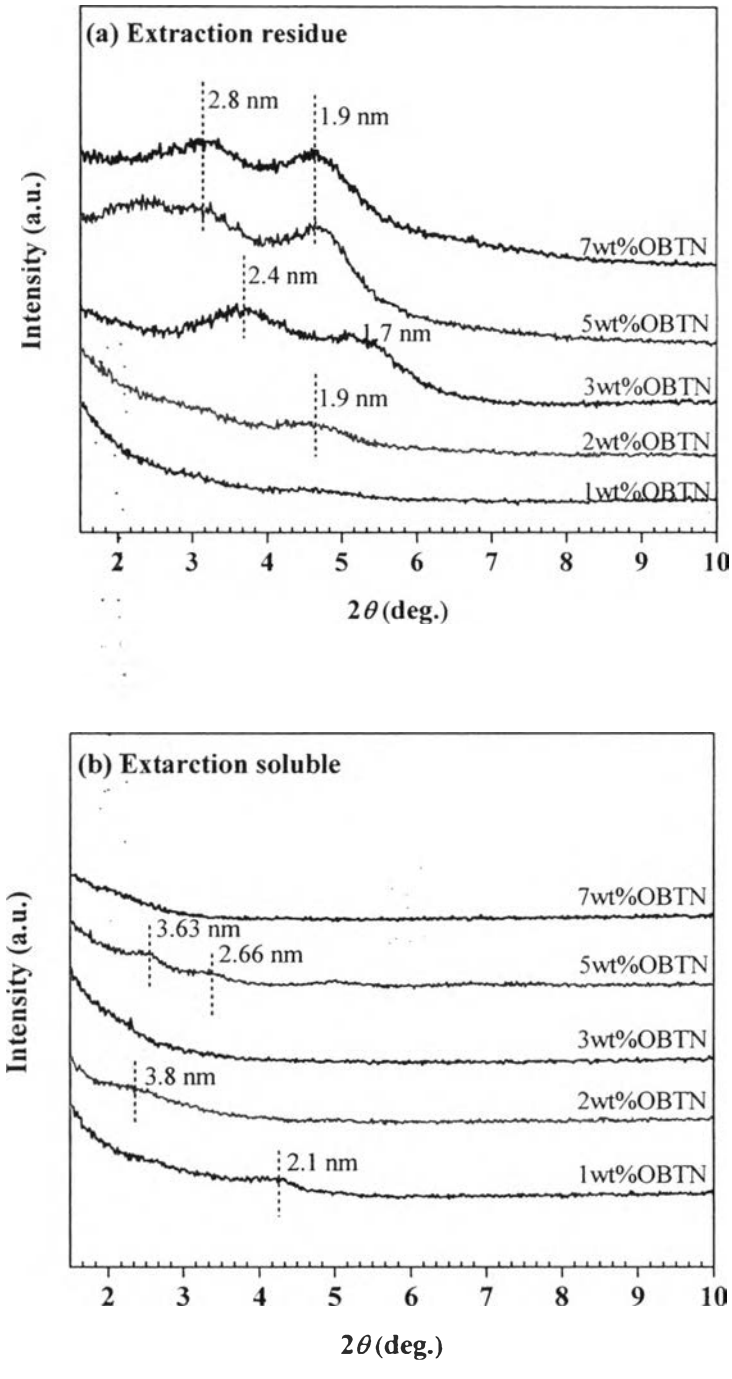

Figure 5.8 XRD patterns of PP/organoclay nanocomposite (a) residue and (b) soluble fractions at various OBTN content.

To more deeply investigate the morphological structure and degree of intercalation, TEM micrographs were collected on the toluene residue and soluble fractions of the 5 wt% OBTN composite and were compared with those collected for the pristine composite material (Figure 5.9(a)–(c)). TEM pictures of the pure composite carried out at low magnification (Figure 5.9(a)) evidenced the presence of submicrometer-sized agglomerates of OBTN, while at high magnification a large number of non-closely packed stacks of a few lamellae was observed. Although a broad size distribution of OBTN agglomerates was evident, the dominant intercalated morphology was consistent with the XRD analysis. Also in the case of residue fractions and toluene soluble fractions, the morphologies observed were in good agreement with the XRD results. In particular, TEM micrographs of the residue fraction at low magnification (Figure 5.9(b)) showed a higher content of inorganic filler with respect to the pristine sample. A high number of sub-micrometric tactoids was observed at low magnification, whereas the high magnification pictures showed isolated platelets and not closely packed stacks of a few lamellae, thus suggesting the presence of polymer chains confined between clay layers. On the other hand, the TEM image of the soluble fraction taken at low magnification (Figure 5.9(c)) showed a very low amount of OBTN dispersed into the polymer matrix. The sample seems to be mainly composed of exfoliated layers with low aspect ratio, even if a small amount of intercalated tactiods is still present, as evidenced by the high magnification picture. This fact further indicates that only a little amount od organoclay particles is not chemically or physically linked to the polymer chains and could be removed by the solvent.

(a) Composite

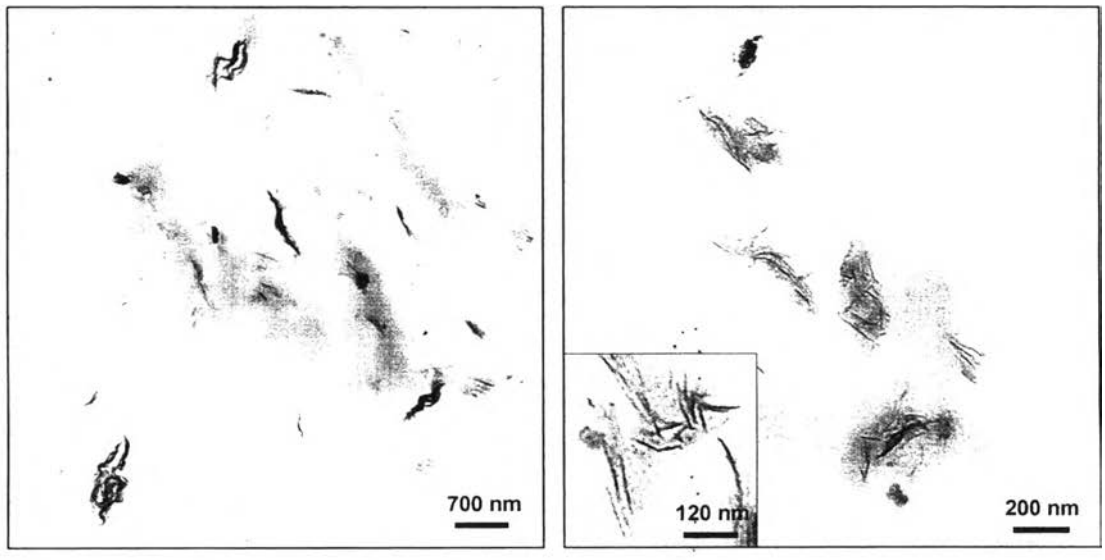

(b) Extraction residue part

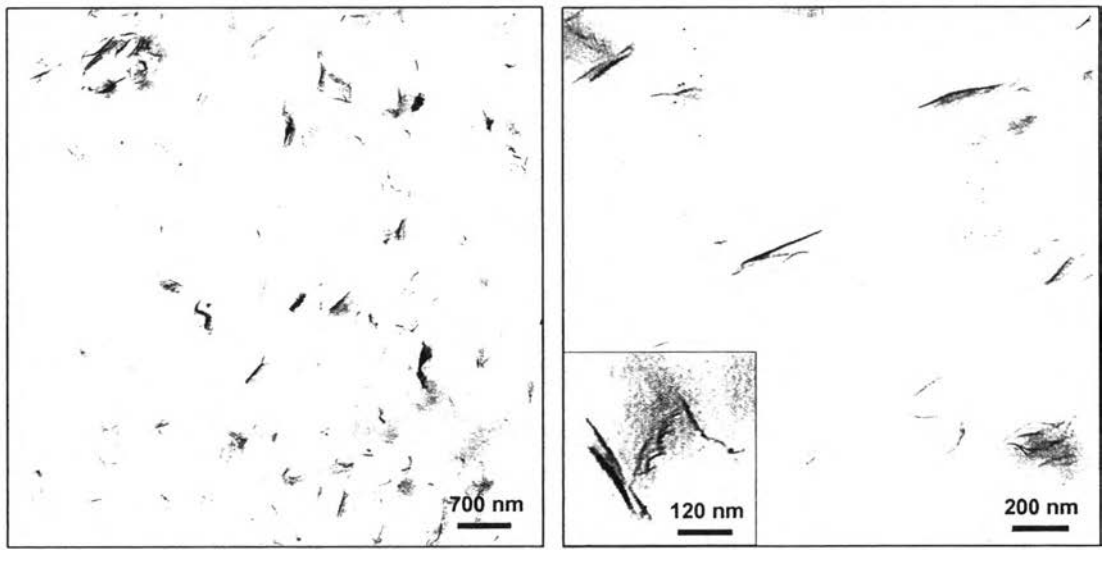

(c) Extraction soluble part

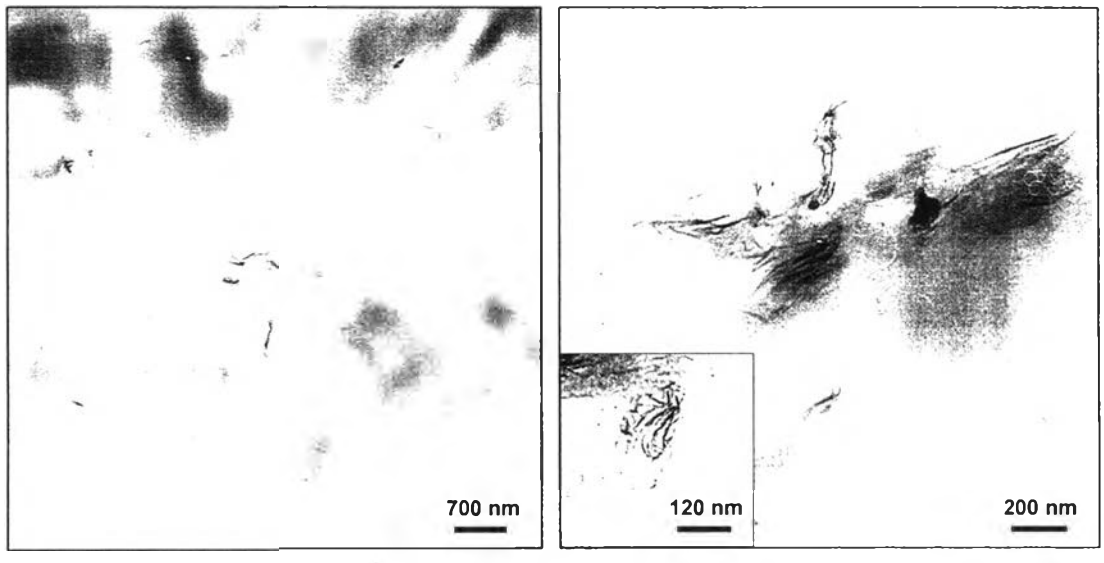

Figure 6.9 TEM micrographs of the 5 wt% PP/organoclay nanocomposite (a) composite, (b) residue fraction, and (c) soluble fraction.

The overall results indicate that toluene extraction process kept unalterated the morphology of composites containing highly disordered structures (1 and 2 wt% OBTN), while markedly changing that of the samples containing the highest concentrations of organoclay (3, 5 and 7 wt% OBTN) and showing an intercalated morphology. This behavior can be attributed to a nonthermodynamically stable dispersion of clay lamellae in the polymer matrix. In fact, it is believed that the exfoliation is promoted by strong interactions between the functional groups present on the compatibilizer polymer chains and the organoclay that favor firstly the intercalation of macromolecules within the galleries and after the delamination of the intercalated structures (Wang *et al.* 2004). Hence, as already stressed by Harrats and Groeninckx, (2008) the intercalation could be considered as an intermediate non-equilibrium step of the process of exfoliation, representing a thermodynamic state of a process forcing polymer chains to enter between two layers of the organoclay without overcoming the energy barrier necessary for completely splitting the layers. A schematic representation of morphologies and the morphological stability to solvent extraction, as dependent on the filler content, is reported in Figure 5.10.

In particular, in the case of the 5 and 7 wt% OBTN composites, during the extraction process, the polymer chains present in between and at the edges of clay layers were removed. As a consequence, after the solvent evaporation, the clay layers in the residues collapsed in parallel stacks or formed percolated structures consisting of several clay layers stacked again. Instead, in the case of 1 and 2 wt% OBTN nanocomposites the exfoliated morphology was maintained and even improved after the extraction.

The TGA analysis of toluene residue and soluble fractions (Table 5.2) showed in the case of 1 and 2 wt% OBTN composites the formation of a comparable amount of inorganic residue (TGA residue at 900°C), as a consequence of an equal partitioning of the clay between the two phases, confirmed by their similar XRD morphology. Most likely, this is due to the good flexibility of the clay layers (Li *et al.* 2003) that can be distorted in the polymer matrix thus easily passing through the holes of the steel net with the solvent. On the other hand, the amount of TGA inorganic residue of the toluene soluble fractions of 3, 5, and 7 wt% OBTN composites was sensibly lower than that of the residue parts: as already indicated by TEM and XRD results. Because of the mainly intercalated morphology of these composites, probably the tactoids/stacks and the percolated structures were hindered to easily pass through the meshes of the metal net used for the extraction, thus remaining in the residual material.

The T_g of the toluene residues (Table 5.2) shifted to higher temperatures compared to that of the unextracted composites. In particular, for the composites prepared by adding 1 and 2 wt% OBTN, respectively, the T_g of the residues was very close to that of the total composites, confirming that in this case the toluene extraction gave only a fractionation by maintaining the same polymer/clay ratio of the pristine material and a similar morphology. On the other hand, in the case of composites prepared with a high OBTN concentration, especially 3 and 7 wt%, an appreciable increase of the T_g of the toluene residues was observed. In this last case, the extraction gave a residue containing mostly polymer-intercalated organoclay and even tactoids having the same interlayer distance of the pure OBTN. The increase of the T_g of the residue can be assigned to the confinement effect of polymer chains between the layers (Passaglia *et al.* 2008).

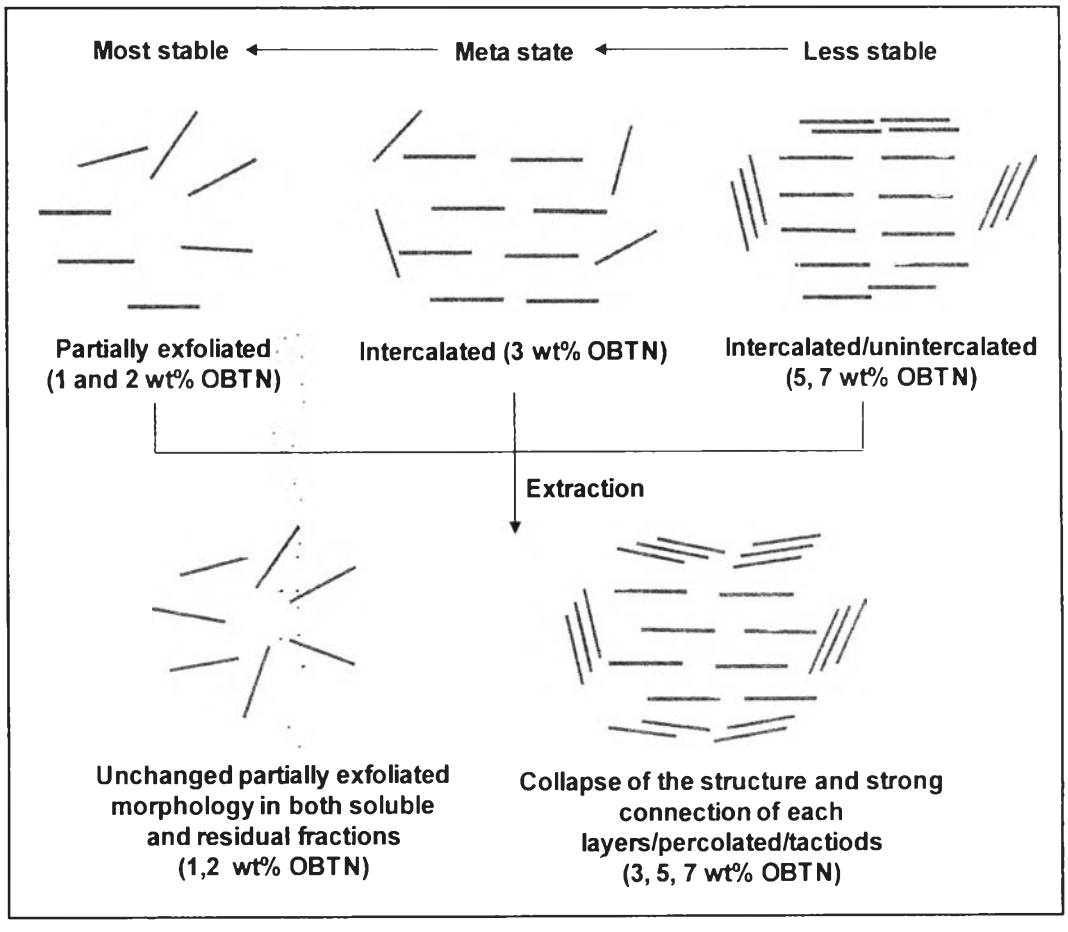

Figure 5.10 Schematic representation of the morphology before and after solvent extraction.

Table 5.2 Xylene and toluene extraction results, % residue, and glass transition temperature of pure PP, PP/PPMAH, and nanocomposites

Composition (PP/PPMAH/Organoclay)	Xylene[a]		Toluene[b]		Char Residue[c] (wt %)		T_g[d] (°C)
	Soluble (wt%)	Residue (wt%)	Soluble (wt%)	Residue (wt%)	Soluble	Residue	
100/0/0	100.0	n.d[e]	74.5	25.5	-	-	-
85/15	100.0	n.d[e]	67.3	32.7	-	-	6.0
84/15/1wt%OBTN	100.0	n.d[e]	60.3	39.7	4.3	2.5	6.5
83/15/2wt%OBTN	100.0	n.d[e]	66.8	33.2	3.9	3.4	9.0
82/15/3wt%OBTN	100.0	n.d[e]	62.6	37.4	1.9	4.8	9.1
80/15/5wt%OBTN	98.7	1.3	50.8	49.2	1.7	7.7	10.0
78/15/7wt%OBTN	95.8	4.2	60.4	39.6	0.5	7.7	8.2

[a] Soluble and residue fractions to the extraction with boiling xylene in Kumagawa for 8 h calculated as percentage of starting material.

[b] Soluble and residue fraction to the extraction with boiling toluene in Kumagawa for 16 h calculated as percentage of starting material.

[c] Char residue at 900 °C for the toluene-soluble fractions and residue fractions obtained from TGA analysis.

[d] Glass transition temperature (T_g) of the toluene-residue fractions of nanocomposites calculated in the range of -10 °C and 30 °C in the second heating curve.

[e] n.d. = not determined

5.4 Conclusions

In this work, the morphology/property relationships of PP nanocomposites containing 1, 2, 3, 5 and 7 wt% organoclay were investigated. The XRD analysis indicated that two distinct groups of nanocomposites were obtained. In particular, samples prepared with lower amounts of organoclay (1 and 2 wt%) provided an exfoliated/intercalated mixed morphology and were characterized by a significant improvement in thermal stability compared to that of the polymer matrix (PP/PPMAH). After the threshold composition of 3 wt% organoclay, the nocomposite morphology moved from quasi-exfoliated to intercalated/unintercalated showing only a minor improvement in thermal properties. The extraction of nanocomposites with hot toluene was carried out to estimate the polymer–clay interactions and it was particularly useful for evaluating the stability of the nanocomposite morphology. Indeed, it was found not only that the solubility in hot toluene depends on the nanocomposite composition and interactions between polymer chains and silicate layers, but also that the solvent is able to differentially split polymer chains and clay layers as a function of the morphology.

The extraction process preserved and in some case improved the morphology of composites having a quasi-exfoliated structure and containing the lower amount of organoclay, thus obtaining two fractions (soluble and insoluble) having similar morphology and polymer/clay ratio. For samples containing the higher organoclay concentration and having an intercalated morphology (3, 5 and 7 wt% organoclay) the same extraction procedure promoted the formation of a residue fraction containing almost the total amount of the clay and showing a collapse of the inorganic structure with a further reduction of the basal spacing. Hence, the solvent was unable to break apart polymer chains and clay layer bundles dispersed tightly within the matrix; on the other hand, the larger amount of intercalated structures were preferentially maintained in the residue fraction and the polymer chains confined between the layers were partially removed by the solvent. In this case, an appreciable increase of the T_g of the residue fraction was observed compared to that of the pristine composite as if the extraction process had selected that fraction where strong interactions between polymer chains and clay layers were formed.